Quad/Octree Adaptive Geophysical Fluid Dynamics

Stéphane Popinet[1], Graham Rickard, Joanne O'Callaghan

National Institute of Water and Atmospheric Research

Wellington, New Zealand

[1]s.popinet@niwa.co.nz

The Gerris Flow Solver

- A framework to solve partial differential equations on quad/octree finite-volume meshes
- Basic blocks: advection–diffusion, Poisson, Helmoltz solvers
- Combination: Euler, Stokes, Navier–Stokes, Saint-Venant etc...
- User-defined tracers, Lagrangian particles, source terms etc...
- Scalable parallel domain decomposition (using MPI)
- Free Software (General Public License): `http://gfs.sf.net`
- 312 registered users: universities, research institutes, industry, independent etc...

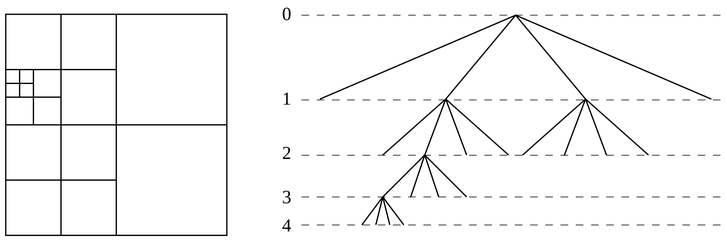

Two-dimensional quadtree spatial discretisation and corresponding logical structure.

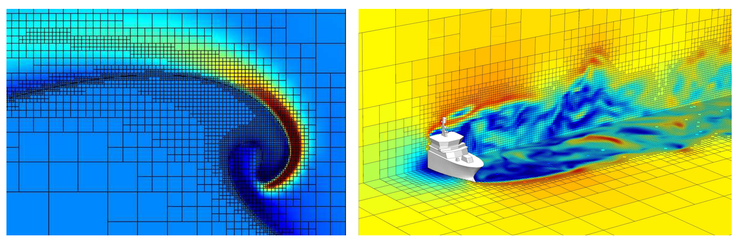

2D adaptive quadtree for incompressible two-phase air–water wave breaking. 3D adaptive octree for incompressible flow with complex solid boundaries.

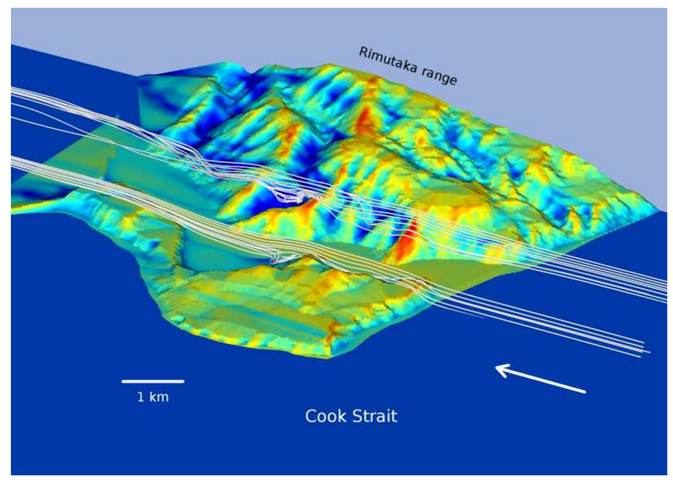

Small-scale turbulent wind flow over steep topography computed using the 3D adaptive octree Navier–Stokes solver. The topography is coloured according to the mean wind speed at wind-turbine height.

Incompressible Navier–Stokes solutions

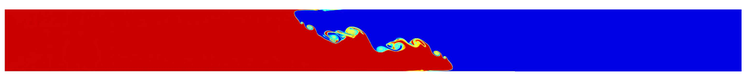

Lock-exchange experiment, density field at $t = 2$.

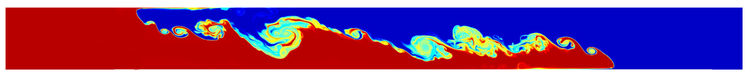

Density field at $t = 6.1$.

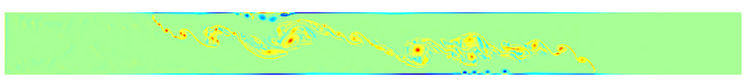

Vorticity field at $t = 6.1$.

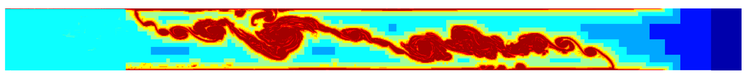

Levels of refinement at $t = 6.1$.

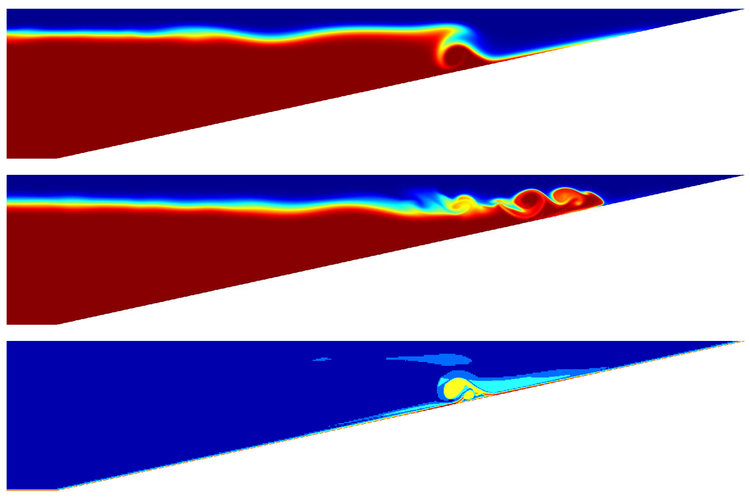

Internal gravity wave breaking on an inclined slope. The top two pictures display the density field at $t = 7.05$ and $t = 9.9$ seconds respectively. Bottom picture displays the level of adaptive refinement at $t = 7.05$. The average gain in mesh size is ≈ 50 compared to an equivalent regular Cartesian grid discretisation.

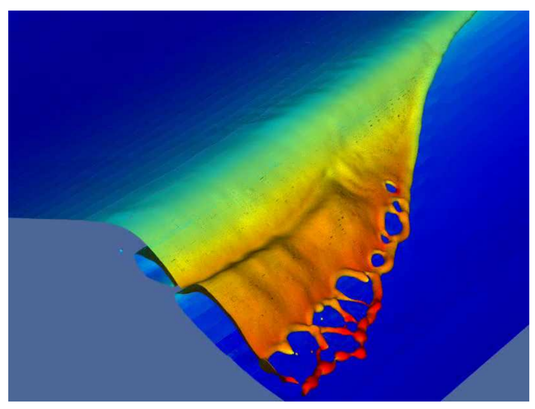

3D direct numerical simulation of a 10 cm air–water breaking wave. Atomisation and spray formation are controlled by surface tension.

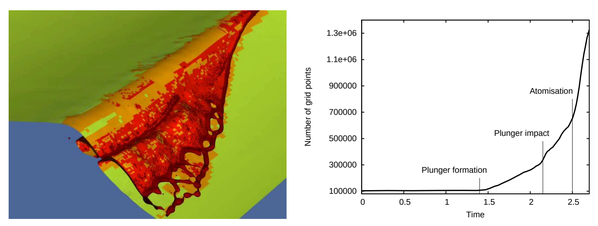

Corresponding level of refinement. The curve on the right is the evolution with time of the number of discretisation elements. An equivalent regular Cartesian mesh would require 10^9 elements.

Shallow-water solutions

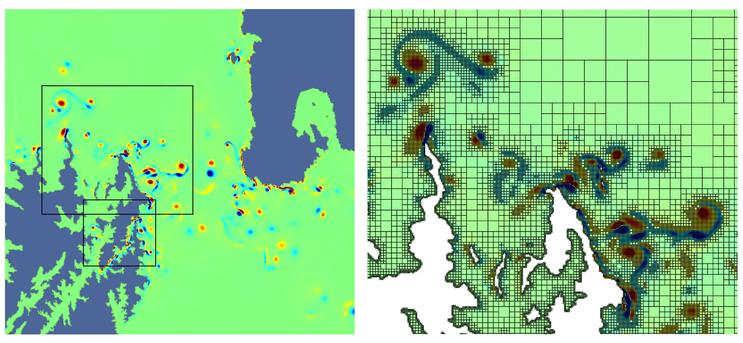

50×50 km detail of tidal flow through Cook Strait, New Zealand. The entire domain is 500×500 km. The colour is vorticity. The right picture displays a detail of the adaptive quadtree mesh. The maximum resolution is 100 metres, decreasing to 10 km offshore.

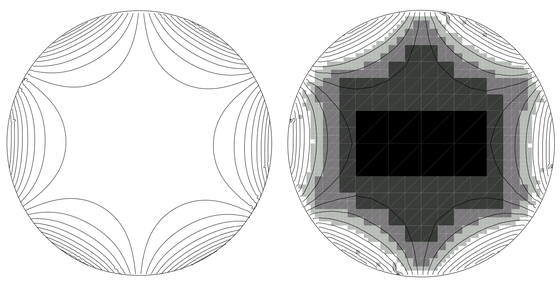

Model	Resolution (km)	Maximum C	Angle of max C (°)
Gerris	37.5	0.9766	3.7
	18.75	0.9904	0.2
	9.375	1.0040	0.0
	4.6875	1.0310	0.0
FVCOM	40	0.9921	-4.6
	20	0.9934	-1.6
	10	0.9993	-0.5
	5	0.9999	-0.2
ROMS	40	0.9801	-35.5
	20	0.9909	-18.2
	10	0.9971	-9.3
	5	0.9986	-4.9

Coastally-trapped inertia–gravity waves in a 1200 km circular basin. The adaptive resolution (top right) varies from 150 (black) to 9.375 km (white). The table shows error convergence with mesh resolution for different solvers.

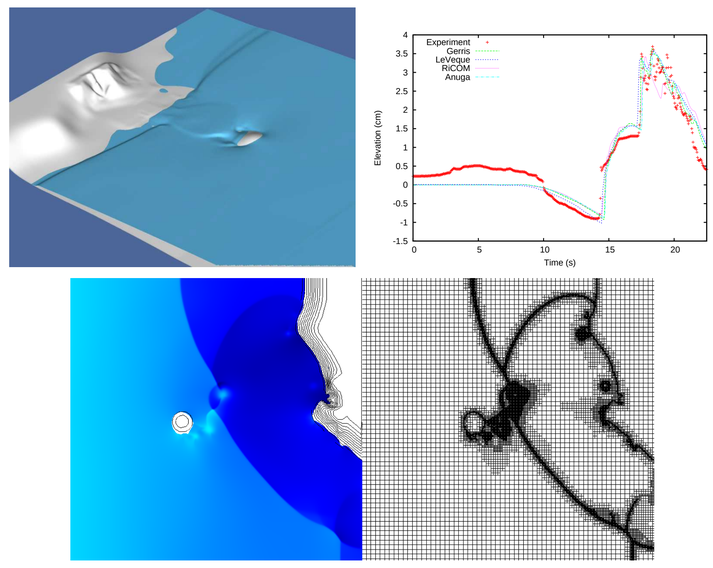

Adaptive tsunami simulation. Okushiri benchmark. The top right curves are the results obtained with different solvers, the symbols represent the experimental data. Bottom picture: adaptivity is based on the slope of the free surface and on the wetting-drying contact line.

Work in progress

Current research applications of the solver regard river plume dynamics and oceanic and atmospheric internal gravity waves.

Extension of the three-dimensional Navier–Stokes solver to large-scale geophysical flows requires the development of efficient solvers for anisotropic Poisson problems. Solutions exist for Cartesian grids but they need to be adapted to adaptive octrees.

We are also developing a general framework for quasi-orthogonal curvilinear mapping of octrees. This will allow octree-adaptive global simulations using spherical mapping (e.g. cubed sphere).

An issue which is rarely discussed in detail is the cost of adaptive methods (per discretisation element) relative to similar schemes implemented on e.g. regular Cartesian grids. We have found that our current octree implementation incurs a factor of ≈ 10 overhead. We are investigating more efficient octree implementations in order to reduce this factor.

References

J. O'Callaghan, G. Rickard, S. Popinet, , and C. Stevens. Assessment of an adaptive model to capture buoyant plume dynamics in a stratified fluid. *Journal of Geophysical Research*, 2009. submitted.

S. Popinet. Gerris: A tree-based adaptive solver for the incompressible Euler equations in complex geometries. *Journal of Computational Physics*, 190(2):572–600, 2003.

S. Popinet. An accurate adaptive solver for surface-tension-driven interfacial flows. *Journal of Computational Physics*, 2009. to appear.

S. Popinet and G. Rickard. A tree-based solver for adaptive ocean modelling. *Ocean Modelling*, (16):224–249, 2007. URL `http://gfs.sf.net/ocean.pdf`.

S. Popinet, M. Smith, and C. Stevens. Experimental and numerical study of the turbulence characteristics of air flow around a research vessel. *J. Ocean. Atm. Tech.*, 21(10):1574–1589, 2004. URL `http://gfs.sf.net/tangaroa.pdf`.

G. Rickard, J. O'Callaghan, and S. Popinet. Numerical simulations of internal solitary waves interacting with uniform slopes using an adaptive model. *Ocean Modelling*, 2009. submitted.

Acknowledgements

Thanks to Murray Smith, Craig Stevens, Luc Deike and Rym Msadek for their contributions to this poster. This work was supported by the Marsden fund of the Royal Society of New Zealand and by the New Zealand Foundation for Research, Science and Technology.